# Coordination of V2G and Distributed Wind Power Using the Storage-like Aggregate PEV Model

Hongcai Zhang, Zechun Hu and Yonghua Song
Department of Electrical Engineering
Tsinghua University, Beijing, China
Email: zechhu@tsinghua.edu.cn

Scott Moura
Department of Civil and Environmental Engineering
University of California, Berkeley, California, USA
Email: smoura@berkeley.edu

***Abstract*—A plug-in electric vehicle (PEV) fleet utilizing vehicle-to-grid (V2G) technology, i.e., a V2G fleet, can behave as a storage system, e.g., promoting integration of distributed wind power resources. However, because the PEVs' behaviors are stochastic and a V2G fleet's population is large, three technical difficulties hinder the utilization of V2G: 1) charging demand forecasting; 2) ahead-of-time charge and discharge scheduling; 3) real-time charge and discharge power dispatching. This paper utilizes a storage-like aggregate model (SLAM) of a V2G fleet that employs aggregated parameters to represent energy and power constraints of the entire PEV population, and therefore reduces the difficulty of forecasting. Then, a stochastic joint power scheduling strategy for a distributed wind generation and a V2G fleet based on the SLAM is proposed aiming to promote the integration of distributed wind power by V2G technology, which has low computational burden. A real-time heuristic strategy is designed to efficiently dispatch the power schedules to PEVs and guarantee the modeling accuracy of SLAM and effectiveness of the proposed power scheduling strategy.**

***Index Terms*—Plug-in electric vehicle, vehicle-to-grid, aggregate model, wind power.**

## I. Introduction

Utilizing V2G technologies, a group of PEVs can form a V2G fleet under the control of an aggregator; this fleet can behave like a storage system, e.g., promoting distributed wind power integration. However, since the PEVs' behaviors are stochastic and their population is large, there are three technical difficulties that hindered large-scale V2G utilization:

1) Charging demand forecasting, which is fundamental for V2G capacity evaluation and requires high accuracy;
2) Ahead-of-time charge and discharge scheduling, which should be able to provide power schedules of the whole PEV population with low computational burden while fully utilize the fleet's V2G capacity;
3) Real-time power dispatching, which should dispatch the charge and discharge power schedules to each PEV efficiently and with low communication burden.

Some researchers studied V2G utilization to promote wind power integration based on individual PEV modeling , which include centralized control strategies [1]–[3] and decentralized control strategies [4]. These works assumed that PEV charging demands could be precisely obtained, which ignored the forecasting difficulty for PEV charging demands. Besides, schedule large-scale PEVs' individual charge and discharge power separately and simultaneously for centralized strategies is computationally expensive. While, though decentralized strategies are computational efficient, it is hard to get optimal results considering the lack of global information.

To overcome the above difficulties, some researchers proposed aggregate models for V2G fleets [5]–[8], which do not require individual charging demand forecasting and power scheduling. These works utilize aggregated energy and power constraints to represent the constraints of the entire PEV population. Since the scales of the aggregated constraints are small and irrelevant with the PEV population, the difficulty for charging demand forecasting is reduced. Besides, the charge and discharge scheduling strategy based on the aggregated constraints has low computational burden. And the scheduled charge and discharge power can be efficiently dispatched to individual PEVs by heuristic strategies. In [5], [6], only unidirectional charging power is considered. Reference [7] extended the work in [5], [6] to V2G cases. In a V2G fleet, there may be some PEVs charging and some other discharging at the same time. Since inefficiency is charge and discharge trajectory-dependent, [7] felt it hard to consider it in V2G cases. The aggregate model in [8] also ignored inefficiency.

In our previous work [9], we modified the aggregate model in [7] to a new storage-like aggregate model (SLAM) for a V2G fleet so that inefficiency can be considered. And we designed a heuristic charging strategy based on charging demand laxities and state-of-charges ($SoC$s) of PEVs (laxity-$SoC$ based strategy) to enhance the modeling accuracy of SLAM. This paper extends [9] and develops a stochastic optimization strategy for joint power scheduling of a distributed wind generation and a V2G fleet based on the SLAM model aiming to smooth the wind power profile and promote wind power integration. Numerical experiments are conducted to verify the effectiveness of the proposed strategy.

## II. Storage-like Aggregate Model

### A. Individual PEV Model

The charging and discharging capacities (V2G capacity) of a given PEV $i$ can be modeled by its energy and power boundaries, i.e., $\{e_i^{+/(-)}, p_i^{+/(-)}\}$, which specify the feasible set of all possible charging/discharging trajectories. The upper

This work was supported in part by the National Natural Science Foundation of China (51477082) and the National Basic Research Program of China (2013CB228202).

energy boundary $e_i^+$ corresponds to the fastest path for consuming energy, whereas the lower boundary $e_i^-$ corresponds to the slowest path for consuming energy. $p_i^+$ is the maximum charging power and $p_i^-$ is the maximum discharging power.

*1) Uncontrollable Charging Demand:* A PEV with an expected parking duration that is not long enough for it to become sufficiently recharged must continue to charge throughout its parking duration. To model the uncontrollable charging demand of PEV $i$, we can simply use the PEV's uncontrollable charging power, i.e., $p_i^{\mathrm{u}}$, instead of its energy and power boundaries, which can be calculated as follows:

$$p_{i,\tau}^{\mathrm{u}} = \begin{cases} 0, \ \tau > t_i^{\mathrm{d}} \text{ or } \tau \le t_i^{\mathrm{a}} \\ p_i^{\mathrm{c}}\eta^{\mathrm{c}}, \ t_i^{\mathrm{a}} < \tau \le t_i^{\mathrm{d}} \end{cases}. \tag{1}$$

where, $t_i^{\mathrm{a}}$ and $t_i^{\mathrm{d}}$ are respectively the arrival time and expected departure time of PEV $i$; $p_i^{\mathrm{c}}$ is PEV $i$'s rated charging power and $\eta^{\mathrm{c}}$ is the charging efficiency; $\tau$ is the time interval index.

*2) Controllable Charging Demand:* A PEV with an expected parking duration that is longer than the required charging time can be recharged from (or discharge to) the grid under the control of an aggregator. To fulfill the customer's regular driving demands and preserve battery life, a PEV should be recharged immediately after connecting to the grid until its $SoC$ reaches a safe minimum threshold $SoC_i^{\min}$. Let $e_i^{\min} = (SoC_i^{\min} - SoC_i^{\mathrm{a}})B_i$ denotes the minimum energy acquired by the battery before it can discharge; $SoC_i^{\mathrm{a}}$ is the PEV's arrival $SoC$ and $B_i$ is its battery capacity.

A PEV $i$ with $e_i^{\min} \le 0$ may charge or discharge throughout its parking duration; its energy and power boundaries are shown in Fig. 1. Its energy boundaries can be calculated using equations (2)–(3) and the corresponding power boundaries can be calculated using equations (4)–(5):

$$e_{i,\tau}^+ = \begin{cases} e_{i,t_i^{\mathrm{d}}}^+, \ \tau > t_i^{\mathrm{d}} \\ \min\left(e_{i,\tau-1}^+ + p_i^{\mathrm{c}}\eta^{\mathrm{c}}\Delta t, e_i^{\max}\right), t_i^{\mathrm{a}} < \tau \le t_i^{\mathrm{d}} \\ 0, \ \tau \le t_i^{\mathrm{a}} \end{cases} \tag{2}$$

$$e_{i,\tau}^- = \begin{cases} e_i^{\mathrm{need}}, \ \tau > t_i^{\mathrm{d}} \\ \max\left(e_{i,\tau-1}^- + p_i^{\mathrm{d}}\Delta t/\eta^{\mathrm{d}}, e_i^{\min}, e_i^{\mathrm{need}} - \right. \\ \qquad \left. p_i^{\mathrm{c}}\eta^{\mathrm{c}}(t_i^{\mathrm{d}} - \tau)\Delta t\right), \ t_i^{\mathrm{a}} < \tau \le t_i^{\mathrm{d}} \\ 0, \ \tau \le t_i^{\mathrm{a}} \end{cases}, \tag{3}$$

$$p_{i,\tau}^+ = \begin{cases} 0, \ \tau > t_i^{\mathrm{d}} \text{ or } \tau \le t_i^{\mathrm{a}} \\ p_i^{\mathrm{c}}\eta^{\mathrm{c}}, \ t_i^{\mathrm{a}} < \tau \le t_i^{\mathrm{d}} \end{cases}, \tag{4}$$

$$p_{i,\tau}^- = \begin{cases} 0, \ \tau > t_i^{\mathrm{d}} \text{ or } \tau \le t_i^{\mathrm{a}} \\ p_i^{\mathrm{d}}/\eta^{\mathrm{d}}, \ t_i^{\mathrm{a}} < \tau \le t_i^{\mathrm{d}} \end{cases}. \tag{5}$$

where, $p_i^{\mathrm{d}}$ is PEV $i$'s rated discharging power and $\eta^{\mathrm{d}}$ is the discharging efficiency; $e_i^{\max} = (100\% - SoC_i^{\mathrm{a}})B_i$ is the maximum energy that can be acquired by the battery; $e_i^{\mathrm{need}} = (SoC_i^{\mathrm{d}} - SoC_i^{\mathrm{a}})B_i$ is the required energy acquired by the battery when the PEV departs; $SoC_i^{\mathrm{d}}$ is the expected departure $SoC$ which depends on the customer's future driving demands; $\Delta t$ is the duration of each sub-hourly time interval.

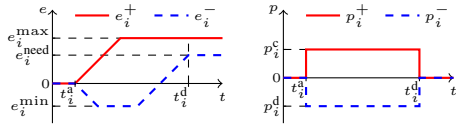

(a) Energy boundaries (b) Power boundaries

Fig. 1. Energy and power boundaries of a controllable PEV with $e_i^{\min} \le 0$.

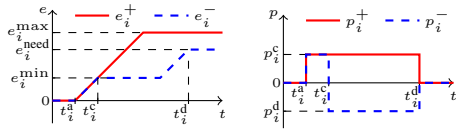

(a) Energy boundaries (b) Power boundaries

Fig. 2. Energy and power boundaries of a controllable PEV with $e_i^{\min} > 0$.

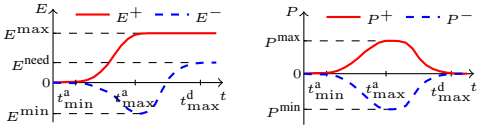

(a) Energy boundaries (b) Power boundaries

Fig. 3. Aggregate controllable energy and power boundaries of a V2G fleet.

A PEV $i$ with $e_i^{\min} > 0$ must be recharged before its $SoC$ reaches $SoC_i^{\min}$ at time $t_i^{\mathrm{c}}$. Thereafter, it may charge or discharge throughout the remaining parking duration. Its energy and power boundaries are demonstrated in Fig. 2. Its uncontrollable charging power before $t_i^{\mathrm{c}}$ can be calculated using equation (1). Its controllable energy and power boundaries after $t_i^{\mathrm{c}}$ can be calculated using (2)–(5).

### *B. Storage-like Aggregate Model of the V2G Fleet*

We utilize the summation of energy and power boundaries of all individual PEVs to represent the V2G fleet's aggregate energy and power boundaries. The aggregate uncontrollable charging power of the V2G fleet can be calculated as follows:

$$P_\tau^{\mathrm{u}} = \sum_i p_{i,\tau}^{\mathrm{u}}, \forall \tau. \tag{6}$$

The aggregate controllable energy and power boundaries of the V2G fleet can be calculated as follows:

$$E_\tau^{+/(-)} = \sum_i e_{i,\tau}^{+/(-)}, \forall \tau, \tag{7}$$

$$P_\tau^{+/(-)} = \sum_i p_{i,\tau}^{+/(-)}, \forall \tau. \tag{8}$$

which specify the feasible set of the controllable part of charging trajectories of the whole V2G fleet. A demonstration of $E^{+/(-)}$ and $P^{+/(-)}$ are shown in Fig. 3.

The set $\{P^{\mathrm{u}}, E^{+/(-)}, P^{+/(-)}\}$ contains the aggregated charging demand and V2G capacity information of the V2G fleet and its scale is independent of the PEV population size.

By the about modeling, we change the large-scale, discrete, randomly distributed individual charging demands into a single, smooth and comparatively steady storage-like aggregate model (SLAM, see Fig. 3). Note that the energy and power boundaries in the proposed SLAM are at the battery side of the V2G fleet; therefore, inefficiency due to charging and discharging has no effect on the SLAM.

Compared with the model in [7], uncontrollable and controllable charging demands are modeled separately in SLAM. Therefore, the charging and discharging power of the V2G fleet can be distinguished and inefficiency can be considered at the grid side, which will be shown in the following sections.

## III. Power Scheduling for A V2G-wind System

Joint power scheduling of distributed renewable power and V2G power may be a promising solution to promote future distributed renewable energy integration. In this paper, we study the strategies of utilizing V2G to promote distributed wind power integration based on SLAM. We assume a V2G fleet and a wind power generation is connected to a distribution system via a distribution transformer to form a V2G-wind system. And the V2G-wind system can purchase or sell electricity from the retailer, while the purchase tariffs and selling prices are time-of-use and fixed.

We develop a stochastic power scheduling strategy for the V2G-wind system in order to maximize the system's benefits. At each time interval, the aggregator optimizes the wind power curtailment and charge and discharge power for the future time intervals based on the forecasted wind power profiles and PEV charging demands (the aggregate energy and power boundaries, i.e., SLAM, of the V2G fleet). In a fleet of PEVs with large population, the stochastic characteristics of individual PEVs will have little influence on the SLAM due to the scale effect [9]. Therefore, in this paper we only consider the uncertainty of wind power generation.

Let $t$ denote the next time interval. Without loss of generality, we use $\{P_\tau^{\mathrm{u}}, E_\tau^{+/-}, P_\tau^{+/-} | \tau = t, ..., t_{\max}^{\mathrm{d}}\}$ to denote the parameters of SLAM. Note that the uncontrollable power $P_\tau^{\mathrm{u}}$ is scenario-independent and cannot be optimized. $t_{\max}^{\mathrm{d}}$ is the maximum expected departure time of all of the involved PEVs. The stochastic power scheduling problem at $t-1$ is formulated as a mixed integer nonlinear programming model:

$$\begin{aligned}\max f = &\sum_{\omega\in\Omega}\sum_{\tau=t}^{t_{\max}^{\mathrm{d}}} \pi_\omega \Delta t \left(-\lambda_\tau^{\mathrm{p}} P_{\omega,\tau}^{\mathrm{p}} + \lambda_\tau^{\mathrm{s}} P_{\omega,\tau}^{\mathrm{s}}\right) \\ &+ \sum_{\omega\in\Omega}\sum_{\tau=t}^{t_{\max}^{\mathrm{d}}} \left(-\pi_\omega \Delta t \lambda^{\mathrm{b}} P_{\omega,\tau}^{\mathrm{ev,d}}\right) \\ &+ \sum_{\omega\in\Omega}\sum_{\tau=t}^{t_{\max}^{\mathrm{d}}} \mu\pi_\omega \left(-P_{\omega,\tau}^{\mathrm{p}} + P_{\omega,\tau}^{\mathrm{s}}\right)^2 \qquad (9)\end{aligned}$$

$$\text{st: } D_{\omega,\tau} P_\tau^- \le P_{\omega,\tau}^{\mathrm{ev,d}} \le 0, \forall\omega, \forall\tau \qquad (10)$$

$$0 \le P_{\omega,\tau}^{\mathrm{ev,c}} \le (1 - D_{\omega,\tau}) P_\tau^+, \forall\omega, \forall\tau \qquad (11)$$

$$P_{\omega,\tau}^{\mathrm{ev,s}} = P_{\omega,\tau}^{\mathrm{ev,d}} + P_{\omega,\tau}^{\mathrm{ev,c}}, \forall\omega, \forall\tau \qquad (12)$$

$$E_\tau^- \le \sum_{k=t}^{\tau} P_{\omega,k}^{\mathrm{ev,s}} \Delta t \le E_\tau^+, \forall\omega, \forall\tau \qquad (13)$$

$$P_{\omega,\tau}^{\mathrm{ev}} = \left(P_\tau^{\mathrm{u}} + P_{\omega,\tau}^{\mathrm{ev,c}}\right)/\eta^{\mathrm{c}} + P_{\omega,\tau}^{\mathrm{ev,d}} \eta^{\mathrm{d}}, \forall\omega, \forall\tau \qquad (14)$$

$$0 \le g_{\omega,\tau} \le g_{\omega,\tau}^{\mathrm{F}}, \forall\omega, \forall\tau \qquad (15)$$

$$P_{\omega,\tau}^{\mathrm{ev}} + P_{\omega,\tau}^{N} = g_{\omega,\tau} + P_{\omega,\tau}^{\mathrm{p}} - P_{\omega,\tau}^{\mathrm{s}}, \forall\omega, \forall\tau \qquad (16)$$

$$0 \le P_{\omega,\tau}^{\mathrm{s}} \le S_{\omega,\tau} C^{\mathrm{p}}, \forall\omega, \forall\tau \qquad (17)$$

$$0 \le P_{\omega,\tau}^{\mathrm{p}} \le (1 - S_{\omega,\tau}) C^{\mathrm{p}}, \forall\omega, \forall\tau \qquad (18)$$

TABLE I
Notations Used in the Power Scheduling Optimization Model

| | |
|---|---|
| $\omega/\Omega$ | Index/set of all the scenarios of wind power generation |
| $\pi_\omega$ | Occurrence probability of scenario $\omega$ |
| $\lambda_\tau^{\mathrm{p/s}}$ | Energy purchase/selling prices at time $\tau$, in \$/kWh |
| $\lambda^{\mathrm{b}}$ | Battery degradation costs due to discharging, in \$/kWh |
| $g_{\omega,\tau}^{\mathrm{F}}$ | Forecasted wind power for scenario $\omega$ at time $\tau$, in kW |
| $\mu$ | Power profile smooth factor, 1e-7 in this paper |
| $P_{\omega,\tau}^{N}$ | Non-deferential load for scenario $\omega$ at time $t$, in kW |
| $C^{\mathrm{p}}$ | Transformer/distribution line capacity of the V2G-wind system |
| $P_{\omega,\tau}^{\mathrm{p/s}}$ | Decision variables for scenario $\omega$, the amount of power to be purchased/sold at time $\tau$, in kW |
| $P_{\omega,\tau}^{\mathrm{ev,c/d}}$ | Decision variables for scenario $\omega$, the amount of power to be charged/discharged at the battery side of the V2G fleet at time $\tau$, in kW |
| $P_{\omega,\tau}^{\mathrm{ev,s}}$ | Decision variables for scenario $\omega$, the power schedule at the battery side of the V2G fleet at time $\tau$, in kW |
| $P_{\omega,\tau}^{\mathrm{ev}}$ | Decision variables for scenario $\omega$, the power schedule at the grid side of the V2G fleet at time $\tau$, in kW |
| $g_{\omega,\tau}$ | Decision variables for scenario $\omega$, the wind power schedule at time $\tau$, in kW |
| $D_{\omega,\tau}$ | Decision variables for scenario $\omega$, $D_{\omega,\tau} = 1$, if the controllable PEVs are discharged; $D_{\omega,\tau} = 0$, otherwise. |
| $S_{\omega,\tau}$ | Decision variables for scenario $\omega$, $S_{\omega,\tau} = 1$, if the system sells electricity to the grid; $S_{\omega,\tau} = 0$, otherwise. |

The first term in objective (9) is the expected average energy purchase costs and selling incomes for all the scenarios. The second term is the expected average battery degradation costs caused by discharging, which is assumed to be proportional to the aggregate discharging energy schedule, as in reference [7]. To smooth the power profiles of the V2G-wind system, the last term is added to penalize load variations.

Equations (10)–(14) are the mathematical formulation of the proposed SLAM. Equations (10)–(11) define the maximum charging and discharging power limits of the V2G fleet. Binary variables $D_{\omega,\tau}$ ensure that charging and discharging will not happen simultaneously in the aggregation of controllable PEVs. Otherwise, they will counteract each other at the grid side and cause undesirable battery degradation and power losses. Note that the controllable PEV charging demands are flexible, they can endure not being charged during time intervals in which the V2G power schedule is negative. Equations (12)–(13) define the energy limits of the V2G fleet. The V2G power schedules at the grid side are calculated using (14). Because charging and discharging power are distinguished, inefficiency can be considered here, which are ignored in [7].

The wind power is limited by (15) and $(g_\omega^{\mathrm{F}}(\tau) - g_\omega(\tau))\Delta t$ is the curtailed wind energy due to limited transformer or distribution line capacities. Equations (16) defines the power balance constraints. Equations (17)–(18) make sure the power of the V2G-wind system can not violate its upper limit and binary variables $S_{\omega,\tau}$ guarantee the system cannot purchase and sell electricity at the same time.

Because the proposed strategy based on SLAM only schedules the aggregate V2G power of the fleet, the scale of the

problem is very small and it can be efficiently solved.

## IV. Real-time Power Dispatch Strategy

During real-time operation at time interval $t$, the system operator judges the operation scenario, i.e., $\omega$, according to the real-time and short-term forecasted wind power of the current time interval, i.e., $g^{\mathrm{R}}_{\omega,t}$. Then the V2G and wind power schedules at $t$ for scenario $\omega$ obtained at $t-1$ by the power scheduling strategy in Section III, i.e., $P^{\mathrm{ev,s}}_{\omega,t}$ and $g_{\omega,t}$, are chosen to be dispatched.

### A. V2G Power Dispatch

To guarantee the modeling accuracy of SLAM and the effectiveness of the power scheduling strategy, we use laxity-$SoC$ based heuristic strategy to dispatch the V2G power schedules to each PEV, which uses laxity of charging demand and $SoC$ to determine charging and discharging priories for the PEVs. The charging demand laxity of PEV $i$, i.e., $L_i$, is:

$$L_i = t^{\mathrm{d}}_i - t - (SoC^{\mathrm{d}}_i - SoC_i)B_i/\left(\eta^{\mathrm{c}} p^{\mathrm{c}}_i \Delta t\right), \qquad (19)$$

which is the difference between the remaining parking duration and the required charging time of PEV $i$ [10]. The larger the value of $L_i$, the more flexibility the PEV has and vice versa.

For PEVs with large values of $L$, the charging demands are not urgent; therefore, they can be discharged, whereas PEVs with small values of $L$ tend to be recharged. And PEVs with high $SoC$s may have limited charging capacities, whereas PEVs with low $SoC$s may have limited discharging capacities. Additionally, PEVs with $L < L_{\min}$ or $SoC < SoC_{\min}$ must be recharged immediately after they are connected to the grid.

We divide PEVs into $M$ groups in the $L$-$SoC$ plane (see Fig. 4). PEVs in groups with lower indices can discharge to the grid. While those in groups with higher indices tend to get recharged from the grid. PEVs in group $M$ are uncontrollable and must get recharged during the next time intervals.

During real-time operation, the aggregator updates charging demands and statuses of PEVs connected to the grid, identify them into specific groups in Fig. 4 and broadcast charging/discharging instructions to them regularly, e.g. every 15 minutes. First, the uncontrolled charging power $P^{\mathrm{u}}_t$ is dispatched to PEVs in group $M$ to satisfy their urgent charging demands. Then, if the controllable power schedule $P^{\mathrm{ev,s}}_{\omega,t} > 0$, dispatch it to PEVs in groups with higher indices, i.e., dispatch the charging power to PEVs in the order of group $M$ to group 1. Otherwise, dispatch the discharging power to PEVs in the order of group 1 to group $M$.

### B. Wind Power Dispatch

Because of forecasting errors, $g^{\mathrm{R}}_{\omega,t}$ may be not equal to the forecasted value when the power schedule is determined, i.e., $g^{\mathrm{F}}_{\omega,t}$. So that the system operator should adjust the wind curtailment according to $g^{\mathrm{R}}_{\omega,t}$. We constrain that the dispatched wind power should be no more than the power schedule, i.e., $g_{\omega,t}$, so that the total power will not violate the capacity limit. Thus, the dispatched wind power is $\min\left(g_{\omega,t}, g^{\mathrm{R}}_{\omega,t}\right)$ and the corresponding wind power curtailment is $\max\left(0, g^{\mathrm{R}}_{\omega,t} - g_{\omega,t}\right)$.

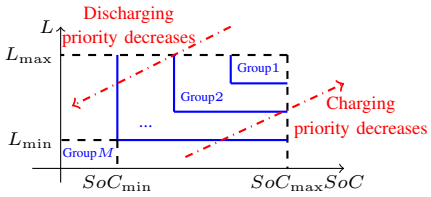


Fig. 4. Classification of PEV groups.

TABLE II
Benchmark Strategies

| Strategy | Model | Charge/discharge Efficiency | Dispatch Strategy |
|---|---|---|---|
| UNC | – | – | Uncoordinated |
| AMLS | AM in [7] | Ignore | Laxity-$SoC$ based |
| SLAML | SLAM | Consider | Laxity based |
| PRO | SLAM | Consider | Laxity-$SoC$ based |

Since the V2G and wind power dispatch strategies are heuristic and require little computational resources, they can be efficiently implemented during real-time operation.

## V. Case Studies

### A. Case Overview and Parameter Settings

We used a V2G-wind system with 1,000 PEVs and 1.2 MW wind generation in a residential area to verify the effectiveness of the proposed method. The Nissan Leaf PEV was chosen to represent the PEV population, with a battery capacity 24 kWh. We assumed 50% of customers installed Level 1 chargers with $P^{\mathrm{c}}$ of 3.3 kW and $P^{\mathrm{d}}$ of -3.3 kW. The others installed Level 2 chargers with $P^{\mathrm{c}}$ of 6.6 kW and $P^{\mathrm{d}}$ of -6.6 kW. The efficiencies ($\eta^{\mathrm{c}}$ and $\eta^{\mathrm{d}}$) were assumed to be 92%. We assumed the non-deferential load for each scenario to be zero[1]. We also assumed $SoC^{\min}_i$=0.4, $M$=10, $\Delta t$=15 min.

We used the charging demand forecasting method in [11] to generate charging demand scenarios, including $t^{\mathrm{a}}_i$, $t^{\mathrm{d}}_i$, $SoC^{\mathrm{a}}_i$, and $SoC^{\mathrm{d}}_i$ of each PEV $i$. We used 10 days' wind speed data in WoNiuShi wind farm in Liaoning, China, to generate 10 wind power scenarios and 5% Gaussian noise is added to represent forecasting errors[2]. Time-of-use electricity tariffs in [6] were used as the electricity purchase costs, and we assumed that the electricity selling prices were 0.02 \$/kWh lower than the corresponding electricity purchase costs. The battery degradation costs was assumed to be 0.078 \$/kWh [6].

The proposed power scheduling strategy (PRO) based on the SLAM was benchmarked with three other strategies (see Table II). In UNC, uncoordinated charging strategy is used and PEVs get charged as soon as they are connected to the grid. In AMLS, the aggregate model (AM) which ignores inefficiency in [6] is used while V2G power schedules are dispatched to PEVs with laxity-$SoC$ based strategy. In SLAML, the SLAM proposed in this paper is used while V2G power schedules are dispatched to PEVs with laxity based strategy.

### B. Simulation Results and Discussions

The average performance of the four strategies are listed in Table III. The total power profiles (selling or purchase), V2G

[1]Note that this will not influence the effectiveness of the proposed strategy.
[2]In practice, the wind power scenarios should be generated based on forecasted wind power profiles and forecasting error analysis.

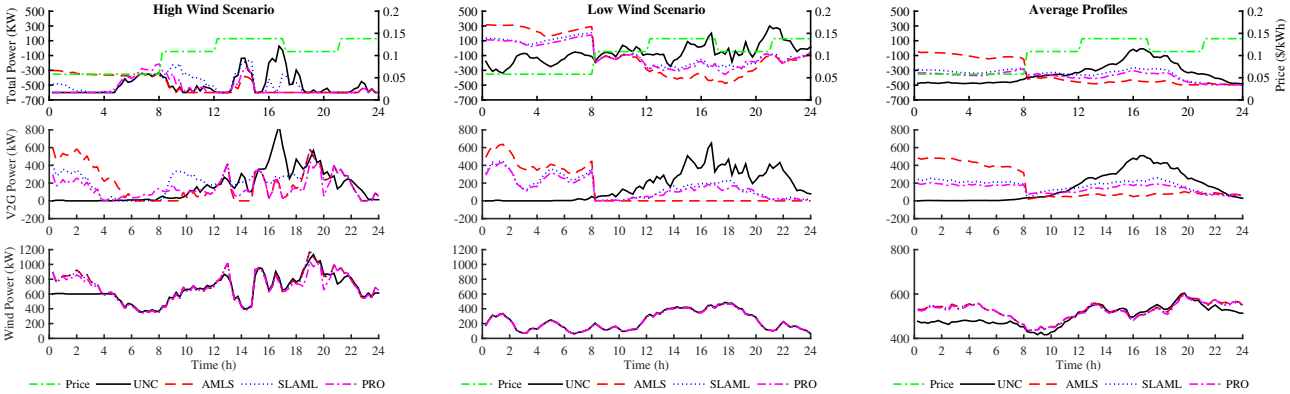


Fig. 5. Simulation results for difference strategies: 1) total power profiles (top); 2) V2G power profiles (middle); 3) wind power profiles (bottom).

TABLE III
PERFORMANCE COMPARISON FOR DIFFERENT STRATEGIES

| Strategy | Energy Selling ($/day) | Energy Purchase ($/day) | Battery ($/day) | Total ($/day) |
|---|---|---|---|---|
| UNC | 645.83 | -47.56 | 0 | 598.27 |
| AMLS | 811.60 | -29.60 | -135.49 | 646.52 |
| SLAML | 720.94 | -11.21 | -5.03 | 704.71 |
| PRO | 774.66 | -6.59 | -10.75 | 757.32 |

power profiles and wind power profiles for two representative scenarios, i.e., high wind scenario and low wind scenario, and the corresponding average profiles for all the scenarios and TOU electricity purchase prices are demonstrated in Fig. 5.

From the simulation results, we can conclude that all the coordinated strategies increase the revenues of the V2G-wind system significantly, while utilizing UNC, a significant amount of wind power are curtailed. In high wind scenario, even though the wind power is higher than the allowed capacity during some period, the extra wind power can be consumed by the V2G fleet and the V2G-wind system can sell much electricity to the grid. While in the low wind scenario, the system has to buy some electricity during low tariff period.

Utilizing AMLS, the V2G fleet is very aggressive in energy arbitraging. On one hand, in AMLS the controllable and uncontrollable charging demands are not distinguished, so that the V2G fleet will be more optimistic with its charging and discharging capacities. And if the schedule V2G power is negative, since there will be some uncontrollable PEVs which have to get charged, the actual discharging power during real-time operation may be higher in order to keep power balance. On the other hand, since inefficiency is ignored, the power scheduling strategy are more aggressive to discharge and recharge the V2G feet since no power losses are calculated. As a results, though the energy selling revenues are high utilizing AMLS, the battery degradation costs increase significantly.

SLAML outperforms AMLS, and the V2G fleet is more moderate in energy arbitrage utilizing SLAM than utilizing AM in [7]. Though energy selling income reduces, the battery degradation costs are saved significantly.

PRO outperforms all the other strategies, and compared with the laxity based strategy in SLAML, the proposed Laxity-SoC based strategy helps to better utilize the flexibility of V2G. The V2G-wind system makes significantly income by selling energy while the battery degradation costs remains low.

## VI. CONCLUSION

A stochastic joint power scheduling strategy for a V2G-wind system is proposed based on the SLAM. A laxity-$SoC$ based heuristic strategy is used to dispatch the V2G power schedules to each PEV during real-time operation. Numerical experiments show that the proposed strategy to be a promising technology to utilize V2G for large-scale PEVs to promote distributed wind power integration which can guarantee high economic performance with low implementation burden.

## REFERENCES


[1] A. Kavousi-Fard, T. Niknam, and M. Fotuhi-Firuzabad, "Stochastic Reconfiguration and Optimal Coordination of V2G Plug-in Electric Vehicles Considering Correlated Wind Power Generation," *IEEE Trans. Sustainable Energy*, vol. 6, no. 3, pp. 822–830, 2015.

[2] H. N. T. Nguyen, C. Zhang, and A. Mahmud, "Optimal Coordination of G2V and V2G to Support Power Grids With High Penetration of Renewable Energy," *IEEE Trans. Transportation Electrification*, vol. 1, no. 2, pp. 188–195, 2015.

[3] D. Wang, X. Guan, J. Wu, J. Wu, P. Li, P. Zan, and H. Xu, "Integrated energy exchange scheduling for multimicrogrid system with electric vehicles," *IEEE Trans. Smart Grid*, pp. 1–13, 2015.

[4] E. L. Karfopoulos, K. A. Panourgias, and N. D. Hatziargyriou, "Distributed Coordination of Electric Vehicles providing V2G Regulation Services," *IEEE Trans. Power Syst.*, vol. 31, no. 1, pp. 329–338, 2015.

[5] S. Vandael, B. Claessens, M. Hommelberg, T. Holvoet, and G. Deconinck, "A scalable three-step approach for demand side management of plug-in hybrid vehicles," *IEEE Trans. Smart Grid*, vol. 4, no. 2, pp. 720–728, 2013.

[6] Z. Xu, W. Su, Z. Hu, Y. Song, and H. Zhang, "A Hierarchical Framework for Coordinated Charging of Plug-In Electric Vehicles in China," *IEEE Trans. Smart Grid*, vol. 7, no. 1, pp. 428–438, 2016.

[7] Z. Xu, D. S. Callaway, Z. Hu, and Y. Song, "Hierarchical Coordination of Heterogeneous Flexible Loads," *IEEE Trans. Power Syst.*, pp. 1–11, 2016.

[8] A. Tavakoli, N. Michael, D. T. Nguyen, and K. M. Muttaqi, "Energy Exchange Between Electric Vehicle Load and Wind Generating Utilities," *IEEE Trans. Power Syst.*, vol. 31, no. 2, pp. 1248–1258, 2016.

[9] H. Zhang, Z. Hu, Z. Xu, and Y. Song, "Evaluation of Achievable Vehicle-to-Grid Capacity Using Aggregate PEV Model," *IEEE Trans. Power Syst. [submitted for publication]*.

[10] A. Subramanian, M. J. Garcia, D. S. Callaway, K. Poolla, and P. Varaiya, "Real-time scheduling of distributed resources," *IEEE Trans. Smart Grid*, vol. 4, no. 4, pp. 2122–2130, 2013.

[11] H. Zhang, Z. Hu, Z. Xu, and Y. Song, "An integrated planning framework for different types of PEV charging facilities in urban area," *IEEE Trans. Smart Grid*, pp. 1–12, 2015.